PHYSICAL REVIEW B **74**, 024108 (2006)

Void lattice formation as a nonequilibrium phase transition

A. A. Semenov and C. H. Woo*
Department of Electronic and Information Engineering, The Hong Kong Polytechnic University, Kowloon, Hong Kong SAR, China
(Received 3 November 2005; revised manuscript received 29 May 2006; published 20 July 2006)

The evolution of a void ensemble in the presence of one-dimensionally migrating self-interstitials is considered, consistently taking into account the nucleation of voids via the stochastic accumulation of vacancies. Including the stochastic fluctuations of the fluxes of mobile defects caused by the random nature of diffusion jumps and cascade initiation, the evolution of the void ensemble is treated using the Fokker-Planck equation approach. A system instability signaling a nonequilibrium phase transition is found to occur when the mean free path of the one-dimensionally moving self-interstitials becomes comparable with the average distance between the voids at a sufficiently high void-number density. Due to the exponential dependence of the void nucleation probability on the net vacancy flux, the nucleation of voids is much more favored at the void lattice positions. Simultaneously, voids initially nucleated at positions where neighboring voids are nonaligned will also shrink away. These two processes leave the aligned voids to form a regular lattice. The shrinkage of nonaligned voids is not a usual thermodynamic effect, but is a kinetic effect caused entirely by the stochastic fluctuations in point-defect fluxes received by the voids. It is shown that the shrinkage of the nonaligned voids, and thus the formation of the void lattice, occurs only if the effective fraction of one-dimensional interstitials is small, less than about 1%. The formation of the void lattice in this way can be accomplished at a void swelling of below 1%, in agreement with experimental observation. The dominance of void nucleation at void-lattice positions practically nullifies the effect of void coalescence induced by the one-dimensional self-interstitial transport.

DOI: 10.1103/PhysRevB.74.024108 PACS number(s): 61.80.Az, 61.80.Hg, 61.72.Cc

I. INTRODUCTION

The formation of void lattices remains a controversial subject without a generally accepted theory for more than thirty years since its first observation.[1] Early theories[2–5] attempt to model void ordering as an equilibrium phase transition via free energy considerations.[6–8] However, the evolution of a void ensemble under irradiation is a far-from-equilibrium dynamical process in an open system, a fact that is recognized by subsequent attempts. The intrinsic difficulty of the next generation of models[9–12] is their orientation degeneracy. These theories cannot account for the observed geometric correlation between the void lattice and the host lattice. Extending[13] one of these models[12] to include the kinetic effect of the intracascade production of glissile self-interstitial clusters introduces the necessary geometrical correlation with the host lattice. However, the theory requires the vacancy clusters to be the dominating point-defect sink,[12,14] which is inconsistent with experimental observations.

Another group of models focuses on the effect of intrinsic anisotropic diffusion of self-interstitial atoms (SIAs).[5,15–18] As a part of their investigation of the effects of anisotropic diffusion on the point-defect kinetics[19] in irradiation damage, Woo and Frank[5,18] explore a possibility suggested by Foreman[15] that crowdions moving one-dimensionally along the close-packed crystallographic directions may introduce a "void shadowing" effect. They construct a quantitative kinetic void-growth model to study the role played by crowdions on the evolution of a system of growing voids. It was found that the resulting system of rate equations does not tend to an asymptotically stationary solution, as usual, but bifurcates. Following sound mechanistic arguments, Woo and Frank[5] hypothesized that the bifurcation can be identified with the instability associated with the nonequilibrium disorder-order phase transition in the system of voids, i.e., the formation of a void lattice. This theory requires that the mean free path λ, which the crowdions travel before converting to three-dimensionally migrating dumbbells, is comparable with the average distance between the voids. In this case, two voids aligned along the close-packed directions share a flux of crowdions generated in the overlapping crowdion-supply cylinders (CSCs) of characteristic length λ. Randomly distributed voids (simply called random or nonaligned voids in the rest of this paper), on the other hand, receive a full flux of crowdions from the unshared CSCs. The reduced interstitial flux received by the aligned voids allows them to grow faster than the random ones. Woo and Frank[5] intuitively postulate that the resulting competition will force the nonaligned voids to shrink away, leaving the aligned voids to form a regular lattice. Indeed, linear stability analysis showed that the homogeneous void distribution becomes unstable when the crowdion mean free path is comparable with the average distance between voids. Emerging from the instability, a periodic structure starts to develop, with symmetry and orientation following that of the host lattice.[5,18] Although the theory sounds plausible, a more detail understanding of the evolution of the void ensemble beyond the bifurcation, and how it leads to the formation of the void lattice, is still necessary to complete the theory.

Following a different approach, Evans used a simplified Monte Carlo simulation, and demonstrated that void lattices may form if interstitials can be assumed to migrate two-dimensionally in the close-packed atomic planes.[16,17] However, such hypothesis lacks experimental support. Nor do molecular dynamic simulations support the existence of the interstitial configurations of SIAs whose migration jumps are

completely restricted to one plane. More importantly, void lattices always form in Evans' model with little exceptions, contrary to experimental observations.

Thus, there is a fairly general consensus that interstitials moving one-dimensionally along the close-packed crystallographic directions are involved in the formation of void lattices, at least they are responsible for the lattice structure and orientation. This is also consistent with the results of molecular dynamic simulations,[20–23] which show that clusters of crowdions can be directly produced in collision cascades and that these clusters can indeed migrate one-dimensionally similar to glissile dislocation loops. The fact that it is the crowdion clusters, but not single crowdions, does not change the essence of the physics underlying the theory of Woo and Frank.[5,18]

Void ordering due to crowdion clusters has also been studied using Monte-Carlo (MC) simulations.[24] It is shown that the crowdion clusters must change the direction of its Burgers vector fairly frequently, so that the mean free path between consecutive changes is less than about two void-lattice nearest-neighbor distances. Otherwise, the void growth characteristics will deviate significantly from those observed experimentally.[24] A more recent MC simulation[25] shows that, even under rather extreme assumptions (very high initial void concentration $\sim 10^{25}$ m^{-3}, and the number of mobile interstitials is 20% higher than the number of mobile vacancies), the mean free path of crowdion clusters has to be about four void lattice nearest neighbor distances in order to produce even a rather poorly defined void lattice (i.e., compared with the experimental ones). A complementary MC study[26] demonstrated that stable void lattice formation by one-dimensional (1D) SIA diffusion mechanism is impeded by the coalescence of neighboring aligned voids. It was also found that void ordering is delayed until the void swelling reaches a value of about 1.5%. Experimentally, however, void lattices are already observable when the swelling is still below 1%.[3,27–29] Based on these results, the causal relationship between 1D self-interstitial transport and the close-to-perfect void lattices observed experimentally is questioned.[26]

There is, however, an obvious inconsistency in the methodology used in the MC simulation.[26] While the inhomogeneous nature of the net vacancy flux in modeling the void growth is fully taken into account, the nucleation of voids, which is essentially the growth of smallest void embryos to the macroscopic size, was assumed to be spatially homogeneous. In reality, the latter assumption was clearly invalid because of the well-known high sensitivity of void nucleation to the magnitude of the net vacancy flux. Indeed, the importance of correct treatment of the void nucleation problem in the understanding of microstructure development has been clearly demonstrated,[30,31] particularly when the microstructure is spatially heterogeneous.

The present paper considers an evolving void ensemble under the mixed fluxes of three-dimensional (3D) isotropically migrating vacancies and mono-self-interstitials, containing a small portion of 1D migrating self-interstitials. There is no artificial separation of the formulation into nucleation and growth regimes. The nucleation of voids via stochastic vacancy accumulation from the smallest embryos and their growth to macroscopic sizes is modeled as one continuous process using the Fokker-Planck equation. Void coalescence due to 1D SIA transport is shown to be unimportant to void-lattice formation, thus removing the concern of the role played by one-dimensional interstitial diffusion in the void-ordering process in this regard.

Since in the majority of cases, such as molybdenum,[28] void lattice formation is observed at temperatures for which vacancy emission from the voids is not important,[32] this contribution is neglected in the present investigation. The paper is organized as follows: In Sec. II, a stochastic model for the kinetics of the nucleation and further evolution of a multicomponent void ensemble under irradiation is formulated, and its properties are investigated. In Sec. III the theory developed in Sec. II is applied to study various characteristics of void-lattice formation caused by 1D interstitial transport due respectively to single crowdion and crowdion clusters, via which the feasibility of the model is assessed. Possible effects of void coalescence are investigated in Sec. IV. The paper is concluded by the discussion of the obtained results.

II. GENERAL FORMULATION

A. Kinetic model

To properly account for void nucleation in the evolution of the void ensemble, the system has to be considered beyond the mean-field approximation in full recognition of the stochastic and nonlinear nature of the problem. In the correct treatment, the number of vacancies in a void is a random (not deterministic) variable that evolves with time, i.e., a stochastic process, which can only be appropriately described by a time-dependent probability distribution. In the simplest approximation, within which the stochastic effects due to the random nature of both the point-defect migratory jumps and cascade initiation can be included, the kinetic equation for the void evolution then takes the form of the Fokker-Planck equation[33]

$$\frac{\partial f(n,t)}{\partial t} = -\frac{\partial}{\partial n}\left\{ V(n) - \frac{\partial}{\partial n} D(n) \right\} f(n,t) + j_0 \delta(n - n_0). \tag{1}$$

Here $f(n,t)$ is the void-density distribution function in the space of void sizes at time t. We measure the size of a void by the number n of vacancies in the void. $V(n)$ is the void growth rate defined by the mean-field theory, and $D(n)$ is the diffusivity that governs the "diffusive spread" of the void distribution function due to stochastic fluctuations. $D(n)$ is related to the average point-defect fluxes and cascade properties and, in the absence of vacancy emission, is given by[33,34]

$$D(n) = \frac{3n^{1/3}}{2a^2}\left(D_\nu C_\nu + D_i C_i\right) + \frac{3GN_d}{4ak}[1 + (1 - \varepsilon_{i0})^2]n^{2/3} \equiv d^s n^{1/3} + d^c n^{2/3}, \tag{2}$$

where D_j and C_j $(j=i, \nu)$ are the diffusion coefficient and the concentration of point defects, respectively, G is the *effective* generation rate of point defects, N_d is the average number of point defects generated in a single cascade, k^2 is the total

sink strength for the three-dimensionally mobile point defects, ε_{i0} is the fraction of the interstitials produced directly in collision cascades, which do not participate in the conventional three-dimensional motion, $a=(3\Omega/4\pi)^{1/3}$, and Ω is the atomic volume. The superscripts s and c refer to the contributions of the stochastic fluctuations due to the random migratory jumps and random cascade initiation, respectively.

Taking into account that small vacancy clusters consisting of two or three vacancies are mobile,[35] and a void shrinking below the minimum size $n_{\min}$ cannot be treated as a void anymore, as well as that total void number density has to be finite, we solve kinetic equation (1) with the zero-boundary conditions

$$f(n=n_{\min},t)=0, \quad f(n\to\infty,t)\to 0. \tag{3}$$

Since the smallest void embryos (microvoids) with sizes $n-n_{\min}\sim 1$ may originate either directly from the collision cascades[22,23] or via the agglomeration of single vacancies, a contribution j_0 due to the homogeneous production of void embryos is added to the right-hand side of the kinetic equation (1). For simplicity, we also assume that the initial sizes of void embryos are the same $(n_0-n_{\min}\sim 1)$, which is reflected by the δ function in Eq. (1).

Since both 1D and 3D migrating point defects are present, the mean-field void growth rate $V(n)$ in Eq. (1) is a sum of two corresponding contributions

$$V(n)=\left.\frac{dn}{dt}\right|_{\text{3D defects}}+\left.\frac{dn}{dt}\right|_{\text{1D defects}}, \tag{4}$$

where

$$\left.\frac{dn}{dt}\right|_{\text{3D defects}}=\frac{3n^{1/3}}{a^2}(D_\nu C_\nu-D_i C_i). \tag{5}$$

The corresponding mean-field balance equations for the three-dimensionally moving vacancies and interstitials at steady state can be written as[36]

$$(1-\varepsilon_\nu')G-D_\nu C_\nu(\rho+k_c^2)=0, \tag{6a}$$

$$(1-\varepsilon_i)G-D_i C_i(Z\rho+k_c^2)=0, \tag{6b}$$

where ε_i is the fraction of mobile interstitials that do not participate in the conventional three-dimensional motion, k_c^2 is the void sink strength, ρ is the total dislocation density, and Z is the reaction constant between dislocations and three-dimensionally moving interstitials. As we shall see in the following, the values of ε_i and ε_{i0} in Eq. (2) are directly proportional, but not necessarily equal, to each other.

The quantity ε_v' in Eq. (6a) is to account for the balance of free vacancies due to the production and dissolution of microvoids

$$\varepsilon_\nu'=n_0 j_0/G-n_{\min}\left[\frac{\partial}{\partial n}\frac{D(n)}{G}f(n,t)\right]_{n=n_{\min}}. \tag{7}$$

It is shown in Appendix A that for the stationary solution of Eq. (1)

$$\varepsilon_\nu'=\frac{(n_0-n_{\min})j_0}{G}>0. \tag{8}$$

Solving Eqs. (6), we obtain from (5) that

$$\left.\frac{dn}{dt}\right|_{\text{3D defects}}=\frac{3n^{1/3}G}{a^2(k_c^2+\rho)}\left(\varepsilon_i+\frac{(1-\varepsilon_i)(Z-1)\rho}{(k_c^2+\rho)}-\varepsilon_v'\right). \tag{9}$$

Since $(Z-1)$ is usually a small fraction, and in the case of the void lattice formation the ratio of the sink strengths ρ/k_c^2 is of the order of 10^{-2},[27,37–39] we may neglect the corresponding term in Eq. (9) temporarily. The effect of dislocation bias on void lattice formation will be reconsidered in a later section.

Considering that the cross section of a spherical void of radius $r=an^{1/3}$ in a given close-packed direction is $\pi r^2/s_\perp$, where $s_\perp$ is the corresponding area of projection of the Wigner-Seitz cell, the contribution of the influx of 1D interstitials to $V(n)$ is given by

$$\left.\frac{dn}{dt}\right|_{\text{1D interstitials}}\propto-\frac{3\varepsilon_i G\Omega}{4as_\perp}n^{2/3}. \tag{10}$$

Note that the relation in (10) implicitly assumes that the mean free path of the 1D interstitials is much larger than the average void radius. Otherwise, their reaction with the voids would obey kinetics similar to that of a three-dimensionally moving point defects.[40]

The contribution to the total void growth rate from Eq. (10) is negative and is proportional to the void surface area, while the contribution from Eq. (9) is positive and is proportional only to the void radius. Thus, at some void size n_s the two contributions are equal and opposite, and void growth saturates. Then, in terms of n_s, the mean-field void growth rate $V(n)$ can be written as

$$V(n)=\frac{3n^{1/3}G\varepsilon_i}{a^2(k_c^2+\rho)}\left(1-\frac{n^{1/3}}{n_s^{1/3}}\right)\equiv\nu n^{1/3}\left(1-\frac{n^{1/3}}{n_s^{1/3}}\right). \tag{11}$$

Although in the following subsections ν and n_s will only be used as probing parameters for assessing the feasibility of the present theory, it is important that n_s remains finite as $\varepsilon_i\to 0$. In this regard, since ε_ν' is positive definite, it does not cause any divergence of n_s, and can be omitted from Eq. (11). Nevertheless, its contribution to the final result can be easily taken into account, simply by substituting $(\varepsilon_i-\varepsilon_\nu')$ for ε_i in the expression for ν. As it will be shown in the Sec. III, such substitution is not actually necessary.

B. Stationary state

In Appendix A, the stationary solution $f(n)$ for $n\geq n_0$ of the kinetic equation (1) subject to the boundary conditions (3) is obtained

$$f(n)=\frac{j_0(n_0-n_{\min})}{D(n)}\exp\left[\int_{n^*}^{n}\frac{V(n')}{D(n')}dn'\right], \tag{12}$$

where $n_{\min}<n^*<n_0$.

Using the expressions of $V(n)$ and $D(n)$ in Eqs. (11) and (2), respectively, the integral in Eq. (12) can be straightforwardly evaluated in terms of the mean-field saturation void size n_s

$$\int V(n)/D(n)dn \equiv I(n/n_s) = I_1(n/n_s) - I_2(n/n_s), \quad (13)$$

where

$$I_1(x) = \frac{3}{2\gamma_c}\left(\frac{\gamma_s}{\gamma_c}\right)^2\left[\left(\frac{\gamma_c}{\gamma_s}x^{1/3} - 1\right)^2 + 2\ln\left(\frac{\gamma_c}{\gamma_s}x^{1/3} + 1\right)\right], \quad (14)$$

$$I_2(x) = \frac{1}{\gamma_c}\left[\left(\frac{\gamma_s}{\gamma_c}\right)^3\left(\frac{\gamma_c}{\gamma_s}x^{1/3} - 1\right)^3 + \frac{3\gamma_s}{2\gamma_c}x^{2/3} - 3\left(\frac{\gamma_s}{\gamma_c}\right)^3 \times\ln\left(\frac{\gamma_c}{\gamma_s}x^{1/3} + 1\right)\right], \quad (15)$$

where γ_s and γ_c are related to d^s and d^c in Eq. (2) according to

$$\gamma_s = \frac{d^s}{\nu n_s} \cong \frac{1}{\varepsilon_i n_s}, \quad (16)$$

$$\gamma_c = \frac{d^c}{\nu n_s^{2/3}} = \frac{akN_d}{4\varepsilon_i n_s^{2/3}}[1 + (1 - \varepsilon_{i0})^2]. \quad (17)$$

The quantities γ_s and γ_c account for the stochastic effects due to the random jumps and random cascade initiation, respectively. The void distribution function in Eq. (11) can then be rewritten as

$$f(n) = \frac{j_0(n_0 - n_{\min})}{\nu n_s^{1/3}}\frac{\chi(n/n_s)}{n_s}, \quad (18)$$

where

$$\chi(x) = \frac{\exp[I(x) - I(n^*/n_s)]}{(\gamma_s x^{1/3} + \gamma_c x^{2/3})} \cong \frac{\exp[I(x) - I(0)]}{(\gamma_s x^{1/3} + \gamma_c x^{2/3})}. \quad (19)$$

In Fig. 1, we plot $\chi(n/n_s)$ as a function of n/n_s for various values of γ_s and γ_c. For small values of γ_s and γ_c, the stationary distribution function has a well defined maximum in the vicinity of the mean-field void saturation size n_s. However, the mean-field description of the void system behavior becomes less and less accurate as the stochastic effects, as measured by γ_s and γ_c, increase. Indeed, the peak of the void-size distribution near the mean-field saturation radius first broadens, and then disappears all together. The void size predicted by the mean-field theory is no longer the most probable. Instead, voids with the size of small void embryos n_0 dominate the ensemble population, associated with a drastic reduction of their mean lifetime. The disappearance of the peak signals the instability of the stationary state and the occurrence of a nonequilibrium phase transformation,[41] which is entirely the result of the stochastic noise in the point-defect fluxes. Note that thermodynamic phase transitions can also be described in a similar way, because it is well-known that the stable phase corresponds to the free-energy minimum, or, in other words, to the peak of the equilibrium distribution.

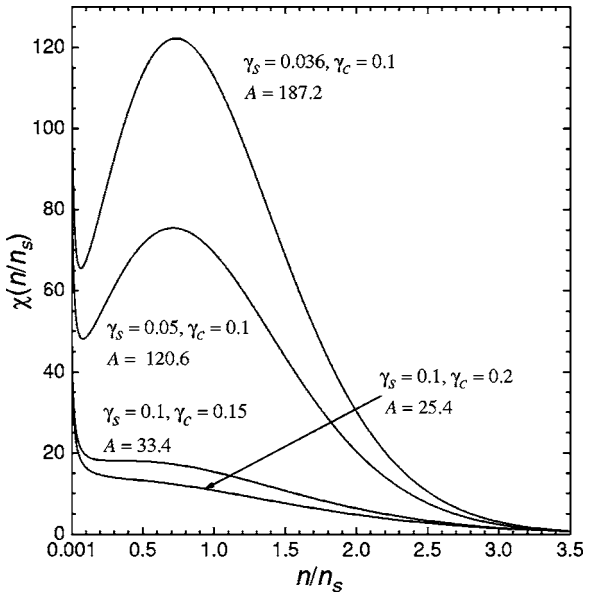

FIG. 1. Void size distribution $\chi(n/n_s)$ for different values of parameters γ_s and γ_c. Here A is the numerically calculated area under the corresponding curve.

A physical picture of this phase transition can be envisioned as follows. In one dimension, the probability of the eventual capture of a random walker by a trap is well known to be unity. Due to the stochastic nature of point-defect fluxes, the growth of a void proceeds such as a random-walk process in the one-dimensional space of void sizes n, but with a positive drift defined by the mean-field growth rate. Since very small vacancy clusters are mobile, a small region near the origin of the space of void sizes can be considered as a "sink," where a shrinking void disappears, i.e., ceases to exist as a separate entity of the void ensemble. Within this picture, every void has a finite mean lifetime before destruction by the stochastic-induced shrinkage, which depends on its size as $n^2/D(n)$. When stochastic fluctuations dominates the kinetics of void growth, most voids exist only for a short period of time due to a large $D(n)$. As a result, few voids can grow to an observable size, and the void-size distribution function maximizes at the size of creation of the smallest voids embryos (Fig. 1). On the other hand, when the characteristic time $n/V(n)$ for the mean-field growth of a void of size n is smaller than the time $n^2/D(n)$ for it to shrink out of existence stochastically, a positive drift is strong enough to drive many voids to grow to observable sizes. These voids will have a long lifetime, and will rarely shrink away. Thus, the disappearance of the peak at the size-distribution function marks a qualitative change in the characteristics of the void ensemble—the fading of the long-life (LL) stable component, and the dominance of the short-life (SL) unstable component.

The LL/SL phase boundary is determined by values of γ_s and γ_c, for which the stationary size distribution (18) is a monotonic decreasing function for all void sizes $n > n_0$. From Eq. (12), this condition is satisfied when

$$\max[V(n) - dD(n)/dn]_{n>n_0} < 0. \tag{20}$$

In terms of γ_s and γ_c and the ratio $x=n/n_s$, this condition can be rewritten as

$$\gamma_s > \max[3x - 3x^{4/3} - 2\gamma_c x^{1/3}]_{x>0}. \tag{21}$$

The value of $x_{\max}>0$, corresponding to the rhs of Eq. (21), is determined by a cubic equation for $x_{\max}^{1/3}$. Treating $2\gamma_c x^{1/3}$ as a perturbation, the positive root of this equation can be very well approximated by the first iteration. As a result, the LL/SL phase boundary can be expressed in terms of γ_s and γ_c by the following equation:

$$\gamma_s = \left(\frac{3}{4}\right)^4 \left(1 - \frac{2^5\gamma_c}{3^4}\right)^3 \left[1 - \frac{2^5\gamma_c}{9(1-2^5\gamma_c/3^4)^2}\right]. \tag{22}$$

C. Multicomponent system

In the context of the present paper, if the ensemble contains more than one subsystem of voids (component), each characterized by a different saturation size, it is crucial to realize that the kinetic equation (1) still applies separately to each component if the total sink strength k^2 includes the total sink strength of all voids in the ensemble. Thus, the interaction among the various components is provided via the total sink strength. This point is central to our present theory. To facilitate comparison of the behaviors of the different components with different saturation radii r_s and $r_{s'}$ we rewrite the phase boundary equation (22) in the form

$$\gamma_s = \beta^3 \left(\frac{3}{4}\right)^4 \left(1 - \frac{2^5\gamma_c}{3^4\beta^2}\right)^3 \left[1 - \frac{2^5\gamma_c}{9\beta^2(1-2^5\gamma_c/3^4\beta^2)^2}\right], \tag{23}$$

where $\beta=r_{s'}/r_s$. In Eq. (23) we take into account that, when the saturation size changes from r_s to $r_{s'}$, the values of γ_s and γ_c are modified by the factors β^{-3} and β^{-2}, respectively.

Thus, for a two-component void ensemble with $\beta=1$ and $\beta=1.4$, for example, the corresponding LL/SL phase boundaries from Eq. (23) are shown in Fig. 2. From Eq. (17), γ_c is seen to be an increasing function of the total sink strength. Then, at the beginning of the radiation when the total sink strength is sufficiently small, both components evolve in the long-life phase, i.e., nucleation and growth of most voids to observable sizes prevail and the system is well described within the mean-field theory. As the irradiation continues, the increasing size and number density of the voids result in a growing *total* sink strength. For a single-component system, the total sink strength saturates. The presence of the higher-β component in a two-component system allows the total sink strength to increase beyond the limit for the single-component system, pushing the system through the $\beta=1$ boundary into a regime where the higher-β component still remains in the long-life phase in which voids of observable size are stable. The lower-β component, on the other hand, is forced to go deeper into the short-life phase in which only a very low density of observable voids can be sustained against stochastic shrinkage. Through this kinetic process, Darwinian selection takes place, resulting in the development of the higher-β component and the suppression of the lower-β component, leading to the eventual dominance of the higher-β component.

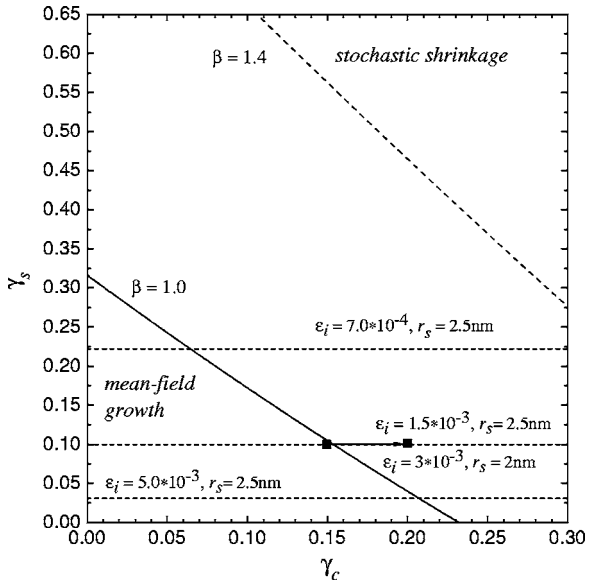

FIG. 2. Phase diagram for the nonequilibrium phase transition in the void ensemble induced by the stochastic fluctuations in point-defect fluxes. The arrow indicates an increase in the value of γ_c with the growth of total sink strength k^2. Dashed lines show the parameter γ_s calculated with the corresponding values of ε_i and r_s.

For a one-subsystem void ensemble, stochastic shrinkage of voids rarely occur because the growth of the void sink strength is limited by the stochastic effect itself. However, if a sufficiently high void number density is achieved, somehow, extra voids of observable sizes are expected to shrink away during further evolution. Such reduction of void number density from an initially overpopulated system of voids of observable sizes is experimentally observable and theoretically demonstrated by both the analytical solution of Fokker-Planck equation[42] and the numerical solution of the time-dependent master equation.[32] Note that, in the absence of any vacancy emission from voids, the void shrinkage is entirely a stochastic effect.[32,42]

During the formation of a void lattice, we have a situation that is quite different from the case of a single-component void ensemble. Indeed, the key point in the Woo-Frank theory[5] of void-lattice formation is that, due to the overlap of diffusion fields, there is a significant reduction in the one-dimensional interstitial flux in the regions where neighboring voids in several close-packed directions are sufficiently close to each other.[5,18] In terms of the present framework, voids nucleated in these reduced interstitial flux (RIF) regions, which we may call RIF voids, have larger saturation sizes in comparison with the "random voids," i.e., voids that do not have close nearest neighbors in the close-packed directions. Considering the void ensemble as a two-component system, in which the RIF voids constitute the higher-β component, and the random voids the lower-β component, the phase transitionlike behavior of void ordering during irradiation can be readily understood via the Darwinian selection process described in the foregoing. In the following, we con-

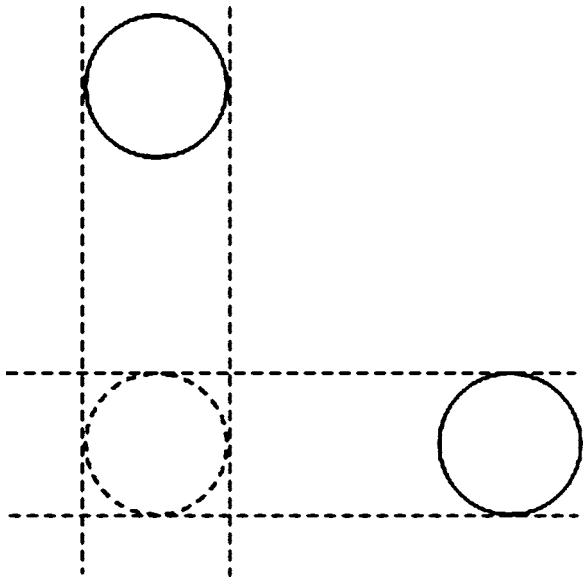

FIG. 3. Schematic diagram showing the area (dashed circle) shaded by two voids, where nucleating void can reach the larger saturation size.

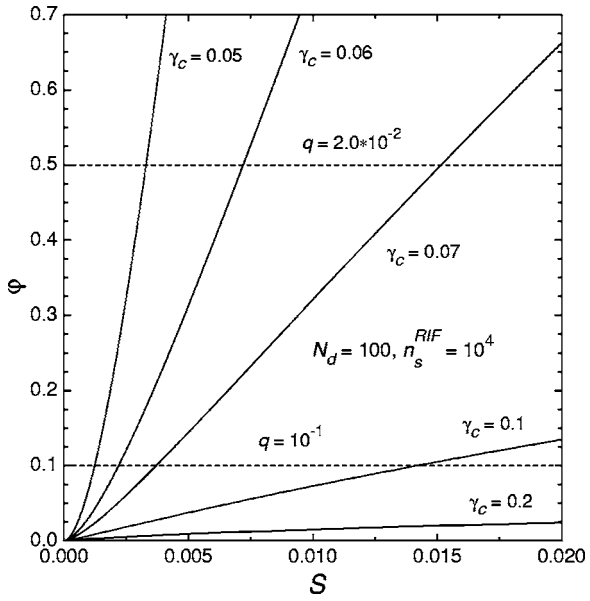

FIG. 4. Function $\varphi(S|\gamma_c)$ given by Eq. (27) at the different values of controlling parameter γ_c. The dashed lines correspond to the right-hand side of Eq. (26). MD simulations for vanadium and iron[23] suggest that in bcc metals the probability for a small immobile three-dimensional vacancy cluster ("microvoid") to be directly formed in a collision cascade may be much less than in fcc copper,[22,23] i.e., $q \ll 1$.

sider the necessary conditions for void ordering within the present theory.

For void ordering to occur, it is clear that the RIF voids must become the dominant void component at some point. Otherwise, the shrinkage of the "excessive" voids would not have much effect other than feeding and stabilizing the growth of the remaining voids, similar to the case of a single subsystem. Each RIF region formed from the intersection of the CSC's is approximately spherical with a radius R equal to the average void radius[5,18] (see Fig. 3). Since the void lattice constant is approximately equal to the average distance between voids, the relative volume occupied by the RIF regions can be approximated by the void swelling S. Using the stationary void-size distribution function given by Eq. (18), the sink strength k^2_{RIF} of the RIF voids for a swelling of S can be estimated

$$k^2_{\mathrm{RIF}} \cong 4\pi S \frac{j_0 a}{\nu\Omega} \int_{n_0/n_s^{\mathrm{RIF}}}^{\infty} \frac{\exp[I(x)-I(0)]}{(\gamma_s+\gamma_c x^{1/3})} dx, \tag{24}$$

where we have assumed $n_0 - n_{\min} \cong 1$. The drift velocity $V(n)$ vanishes at $n=n_s^{\mathrm{RIF}}$, the saturation RIF void size, so that the function $I(x)$ has a maximum at $x=1$. Expanding this function up to the second nonzero term in the vicinity of its maximum and taking into account the definition of the parameter ν in Eq. (11) and γ_s in Eq. (16), we may write

$$\frac{k^2_{\mathrm{RIF}}}{k_c^2} \cong \frac{j_0 n_s^{\mathrm{RIF}}}{G} \frac{\sqrt{6\pi\gamma_c}\exp[\tilde{I}(\gamma_s/\gamma_c)/\gamma_c]}{\sqrt{(\gamma_c/\gamma_s)(1+\gamma_c/\gamma_s)}} S, \tag{25}$$

where $\tilde{I}(\gamma_s/\gamma_c)=\gamma_c[I_1(1)-I_2(1)-I_1(0)+I_2(0)]$. If q is the formation probability of a small immobile three-dimensional vacancy cluster in a collision cascade, then, neglecting the formation of the void embryos through the consecutive agglomeration of single vacancies, the spatially homogeneous rate of generation of the void embryos j_0 is given by qG/N_d. Using Eq. (25), the condition for the RIF voids to be the dominant point-defect sinks, i.e., $k^2_{\mathrm{RIF}}/k_c^2 \cong 1$, can be written in the form

$$\varphi(S|\gamma_c) \cong \frac{N_d}{q n_s^{\mathrm{RIF}}}, \tag{26}$$

where

$$\varphi(S|\gamma_c) \equiv \frac{\sqrt{6\pi\gamma_c}\exp[\tilde{I}(\gamma_s/\gamma_c)/\gamma_c]}{\sqrt{(\gamma_c/\gamma_s)(1+\gamma_c/\gamma_s)}} S. \tag{27}$$

Note that according to Eqs. (14) and (15), the integral $\tilde{I}$ depends only on the ratio γ_s/γ_c, which can be expressed in terms of S

$$\frac{\gamma_c}{\gamma_s} = \frac{r_s^{\mathrm{RIF}} k_c N_d}{4}\left[1+(1-\varepsilon_{i0})^2\right] \cong \frac{\sqrt{3S}N_d}{4}\left[1+(1-\varepsilon_{i0})^2\right], \tag{28}$$

if the RIF voids are the dominant sinks. As a result, the solution of Eq. (26) defines γ_c as a function of S, which must be satisfied as a necessary condition for void ordering. Function φ given by expression (27) is plotted in Fig. 4 as a function of S for various values of γ_c. From this plot, the relation between S and γ_c for various values of q can be read off. For $q=0.1$, for example, if the void lattice is to form at a swelling below 1%, as is often observed experimentally,[3,27,28] the value of γ_c for the RIF component has to be somewhere between 0.06 and 0.07. In addition, if the observable random voids are to start shrinking away, the cor-

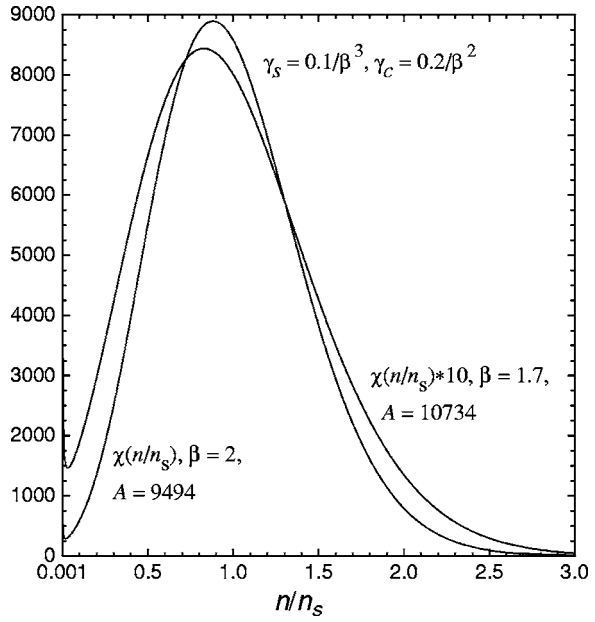

FIG. 5. Void size distribution $\chi(n/n_s)$ in the void subsystems with higher saturation radius (β=1.7 and β=2.0).

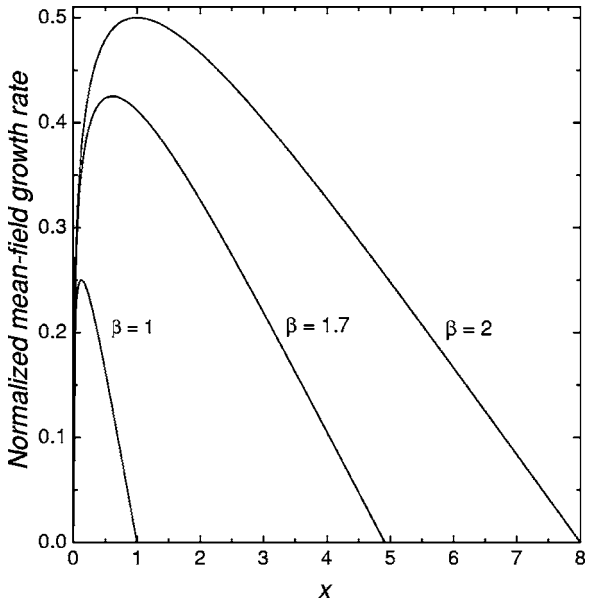

FIG. 6. Normalized mean-field void growth rate $x^{1/3}(1-x^{1/3}/\beta)$.

responding γ_c must have a value larger than ~0.2, (see Figs. 1 and 2), from which we may deduce a value of $\beta \approx (0.2/0.065)^{1/2} \approx 1.7$ for the RIF component. The void-size distribution function for the RIF component is presented in Fig.5 for values of β=1.7 and β=2. Comparing this with the void size distribution function of the random voids (the γ_c =0.2 case in Fig. 1), the large difference in the size distributions for the two components is clear. Indeed, the most easily discernable feature is the two orders of magnitude difference in the scales on the y-axes of the two graphs. This translates into a 400 times difference in the total void-number densities given by the areas under the size distribution functions A in the two graphs. For the number densities of experimentally observable voids the difference is even larger. Thus, even if the total RIF volume is smaller than 1% of the total volume ($S \leq 1\%$), the probability of void nucleation in this volume can still be higher than outside of it.

For a well-defined void lattice to show up, at least a large majority of the observable random voids must disappear, if not all. In other words, the random voids have to be in the SL phase regime, i.e., the corresponding γ_c must satisfy the condition, $\gamma_c > \gamma_c^{cr}$. Using Eq. (17), this condition can be expressed as

$$\gamma_c \cong \left(\frac{a}{r_s}\right)^3 \sqrt{4\pi r_s^{\mathrm{RIF}} N_{\mathrm{RIF}}^{1/3}} \frac{N_d (r_s N_{\mathrm{RIF}}^{1/3})}{4\varepsilon_i} [1 + (1-\varepsilon_{i0})^2] > \gamma_c^{cr}, \tag{29}$$

where N_{RIF} is the concentration of the RIF voids. Estimating N_{RIF} by the density of the aligned voids, we have typically $r_s^{\mathrm{RIF}} N_{\mathrm{RIF}}^{1/3} \simeq 10^{-1}$, $a/r_s \simeq 10^{-1}$, and $N_d \cong 100$. Assuming $r_s^{\mathrm{RIF}} \approx 2r_s$, i.e., $\beta \approx 2$, Eq. (29) becomes

$$\gamma_c \approx \frac{2.8 \times 10^{-3}}{\varepsilon_i} > \gamma_c^{cr}. \tag{30}$$

Using a value of $\gamma_c^{cr} \approx 0.2$, the stochastic shrinkage of the random voids puts an upper limit of ~1% to ε_i, the effective fraction of 1D interstitials. If this fraction is much larger than 1% (note that in the Monte Carlo simulations[24–26] ε_i =100%), the net vacancy flux received by the small random voids would be much higher [see Eq. (11) and Fig. 6]. This means their shrinkage cannot be driven effectively by the stochastic fluctuations, particularly in the absence of vacancy emission. As discussed in the Introduction void ordering is difficult in this case. In this regard, it is interesting to note that molecular dynamics simulations of cascades in bcc vanadium[43] and fcc aluminum[44] show very little intracascade interstitial clustering, including those clusters that undergo 3D migration, such as the di-interstitials.

In molybdenum the total fraction of clustered interstitials in the molecular dynamics (MD) simulations is found to be about 50%.[45] However, most of the clusters produced in 20 and 30 keV cascades are di- and tri-interstitials, the morphology of which is ill defined but shows sessile features.[45] Only clusters of five and more interstitials have structures comparable to prismatic loop embryos, which may be assumed to be mobile. However, few of such clusters are actually produced in the cascades. Thus, in molybdenum the effective fraction ε_i of mobile interstitials with mean free paths much larger than the average void radius is in reality much smaller than the total interstitial clustering fraction. This conclusion is also supported by existing void swelling data in molybdenum.

Indeed, from Eqs. (9) and (11), it can be seen that the mean-field growth rate of small voids is totally determined by the 3D point-defect fluxes. Since molybdenum is characterized by an extremely high void nucleation rate, voids are usually the main sinks for point defects. As a result, the void swelling rate $dS/d(Kt) \geq \varepsilon_i G/K$, where K is the nominal NRT displacement per atom (dpa) rate. Experimentally, even for the voids with the radii as small as 1–2 nm the average swelling rate S/Kt is less than 3×10^{-3}/NRT dpa,[27] which is translated into $\varepsilon_i \leq 10^{-2}$ ($G/K \cong 0.3$,[45]). In the following sec-

tion, where the specific modes of one-dimensional interstitial transport are considered, it will be shown that the assumption of much larger values of ε_i (e.g., $\varepsilon_i \sim 100\%$) will put conditions on the kinetics of the void ensemble inconsistent with experimental observations.

Concluding this section, we would also like to note the following. The quantity γ_c, which accounts for the stochastic effects due to the random cascade initiation, is determined by the ratio of the diffusivity d^c to the net vacancy flux [Eq. (17)]. Since the typical average swelling rate during void lattice formation is about equal to or below 0.1%/NRT dpa, stochastic fluctuations cannot be neglected when considering void lattice formation. This conclusion immediately clear if the term ε_i in Eq. (29) is substituted by S/Gt.

III. VOID-LATTICE FORMATION DUE TO 1D DIFFUSION OF SELF-INTERSTITIALS

In this section we assess the feasibility of the model developed in the foregoing in relation to the specifics of 1D SIA transport, as well as the effect of dislocation bias.

The capture probability P_a for a 1D random walker between the two traps is calculated in Appendix B. Averaged over the initial position of the 1D diffuser, this probability is the same for each trap, and is given by

$$P_a = \frac{\lambda}{l}\tanh(l/2\lambda), \tag{31}$$

where l is the distance between the traps, $\lambda=(D_1\tau_c)^{1/2}$ is the mean free path of the random walker, and D_1 and τ_c are its one-dimensional diffusion coefficient and the mean lifetime, respectively. The latter can be the mean lifetime of the crowdions between their creation and conversion to dumbbells,[5,18] or the average duration between consecutive changes of the Burgers vector of the interstitial clusters.[24]

For an ensemble of random voids, the mean distance λ_1 between two voids along the close-pack directions is equal to $2/\pi R^2 N$.[46] For a void swelling $S=4\pi R^3 N/3$ of less than 1%, $\lambda_1=(2/\pi^{1/3})(4/3S)^{2/3}N^{-1/3}$ is much larger than the average 3D separation $N^{-1/3}$ between the voids. In the following we assume that the mean free path λ of the one-dimensional random walkers is comparable with the average distance $N^{-1/3}$ between voids, and, consequently, much smaller than λ_1. Thus, for the random voids, Eq. (31) dictates $P_a \cong \lambda/l$. As a result, these voids absorbs practically all the one-dimensionally migrating interstitials generated in its interstitial supply cylinders of characteristic length λ. On the other hand, voids aligned along the close-packed directions with overlapping supply cylinders receive a reduced flux of 1D self-interstitials [$\tanh(l/2\lambda)=0.46$ at $l=\lambda$], and grow faster than the random voids. In terms of the description of the last section, these are the RIF voids. The flux of 1D interstitials received by the RIF voids from the supply cylinders depends on the specifics of the reaction kinetics of the 1D self-interstitial, which we will consider in the following sections.

A. Single crowdions

The rate of production of crowdions moving along a given close-packed crystallographic direction is equal to $\varepsilon_{i0}Gs_\perp/\Omega M$, where $\varepsilon_{i0}G$ is the atomic rate of crowdion generation and M is the number of different close-packed directions of the crystal. Thus, the flux of static crowdions, i.e., metastable interstitials that undergoes thermal conversion to the stable dumbbells,[5,18] can be obtained directly from Eq. (31), and Eq. (10) becomes

$$\left.\frac{dn}{dt}\right|_{\text{1D interstitials}} = -\frac{2\pi r^2 \lambda \varepsilon_{i0} G}{\Omega}\Phi = -\frac{3\lambda\varepsilon_{i0}G}{2a}n^{2/3}\Phi. \tag{32}$$

Here $\Phi=1$ for the random voids and $\Phi=\Phi_{\text{RIF}}$ for the RIF voids, with

$$\Phi_{\text{RIF}} = \frac{((2M-m)\tanh(L/\lambda)+m\tanh(L/2\lambda))}{2M}, \tag{33}$$

where L is the nearest-neighbor distance in the void lattice, and m is the average number of nearest void-lattice sites occupied by a void. In Eq. (33) we have also assumed that if the void is not in the CSCs of its nearest neighbors, then it is in the CSCs of the corresponding next nearest neighbors. We note that Φ_{RIF} generally has a value of less than 1, representing a reduction in the interstitial flux, and Φ_{RIF} decreases with decreasing L/λ in general. Accordingly, the fraction of interstitials that do not participate in the conventional three-dimensional motion, i.e., ε_i in Eq. (6), can be expressed in terms of the corresponding fraction ε_{i0} of crowdions produced directly in the collision cascades

$$\varepsilon_i = 2\pi\lambda\varepsilon_{i0}[N_{\text{RIF}}\bar{r}^2_{\text{RIF}}\Phi_{\text{RIF}} + N_{\text{RD}}\bar{r}^2_{\text{RD}} + \rho d/4]. \tag{34}$$

In Eq. (34), N_{RD} is the concentration of random voids, $\bar{r}^2_{\text{RIF}}$ and $\bar{r}^2_{\text{RD}}$ are respectively the average square radii of aligned and random voids, and d is the effective diameter of the absorption cross section of crowdions by dislocations.

Using Eqs. (9), (32), and (34), the mean-field void growth rate is given by

$$\frac{dn}{dt} = \frac{3n^{1/3}G}{a^2k^2}\left(\frac{(1-\varepsilon_i)(Z-1)\rho}{k^2} - \varepsilon'_\nu + \varepsilon_i\left[1 - \frac{k^2 a n^{1/3}\Phi}{4\pi(N_{\text{RIF}}\bar{r}^2_{\text{RIF}}\Phi_{\text{RIF}} + N_{\text{RD}}\bar{r}^2_{\text{RD}} + \rho d/4)}\right]\right) \tag{35}$$

Since the dislocation bias $(Z-1)\sim 10^{-1}$, $\varepsilon'_v \cong q(n_0 - n_{\min})/N_d \sim 10^{-3}$, and ε_i has to be less than 10^{-2}, Eq. (35) can be directly compared with Eq. (11) if and only if the sink strength of the voids is much higher than the density of dislocations, or more precisely, $\rho/k_c^2 \sim 10^{-2}$. In this case, the dominant term is in the square brackets, referring to the void growth essentially at the expense of each other (i.e., void coarsening). Under this condition, the evolution of the void ensemble according to Eq. (35) mirrors that governed by Eq. (11), which has been described in detail in Sec. II. Indeed, the corresponding saturation radius r_s of the random voids is given by

$$r_s = an_s^{1/3} = 4\pi(N_{\mathrm{RIF}}\bar{r}_{\mathrm{RIF}}^2\Phi_{\mathrm{RIF}} + N_{\mathrm{RD}}\bar{r}_{\mathrm{RD}}^2 + \rho d/4)/k^2 \cong \frac{N_{\mathrm{RIF}}\bar{r}_{\mathrm{RIF}}^2\Phi_{\mathrm{RIF}} + N_{\mathrm{RD}}\bar{r}_{\mathrm{RD}}^2}{N_{\mathrm{RIF}}r_{\mathrm{RIF}} + N_{\mathrm{RD}}r_{\mathrm{RD}}}, \tag{36}$$

where r_{RIF} and r_{RD} are the average radii for the RIF and random voids, respectively, and β is equal to Φ_{RIF}^{-1}.

Thus, in the present model, void ordering occurs only if the condition $\rho/k_c^2 \sim 10^{-2}$ is satisfied. Otherwise, conventional bias-driven growth of random voids takes place. This description is consistent with experimental observations in neutron-irradiated niobium. Thus, for pure Nb and Nb-1% Zr, where $\rho/k_c^2 \geq 10^{-1}$, conventional growth of randomly distributed voids is observed.[47] Void lattices are observed only in oxygen doped samples with the void number density that is an order of magnitude higher than in pure Nb under similar conditions.[48]

The foregoing analysis suggests the following picture of void-lattice formation. Initially, the nucleation and growth of randomly distributed voids takes place under the action of the dislocation bias. As irradiation proceeds, void density can indeed reach experimental values at which void lattices can be observed (i.e., up to $N \approx 10^{23}$ m^{-3}) within just a few NRT dpa.[42] At this point, when the sink-strength ratio ρ/k_c^2 drops to about 10^{-2}, the kinetics of the void ensemble changes and becomes dominated by stochastic void coarsening, resulting in the shrinkage and disappearance of the random voids, leaving the RIF voids in a regular lattice positions. The value of the sink strength ratio at which void ordering takes place is also in agreement with the experimental observations.[27,37–39]

In bcc and fcc void lattices, the concentration of voids is equal to (m/ML_0^3) and $2(m/ML_0^3)$, respectively, where L_0 is the void lattice constant, and the ratio $m/2M$ takes into account the imperfect occupancy of the void lattice. For a bcc lattice, for example, ε_i can be estimated as

$$\varepsilon_i \approx 4\pi\varepsilon_{i0}\frac{\lambda}{L_0}\frac{\bar{r}_{\mathrm{RIF}}^2}{L_0^2}\left(\frac{m}{2M}\right)\Phi_{\mathrm{RIF}}. \tag{37}$$

For typical values of the ratios $\bar{r}_{\mathrm{RIF}}^2/L_0^2 \approx 10^{-2}$ and $\lambda/L_0 \approx 1$, and a void-lattice occupancy of about 70%,[49] we have $\varepsilon_i \approx 4.5\times 10^{-2}\varepsilon_{i0}$ ($\Phi_{\mathrm{RIF}} \cong 0.5$ in this case). It then follows from Eq. (30) that for the random voids to start shrinking, the fraction ε_{i0} of the crowdions directly produced in collision cascades and with mean free paths comparable with the average distance between voids, should not exceed about 10%.

The characteristic time scale for lattice formation (from start to finish) can also be estimated. Since void shrinkage occurs through a diffusionlike process in the void size space, the characteristic time t_{cs} of the coarsening process can be estimated from the following diffusion relation:

$$n_s^2 \approx 2D(n_s)t_{cs}(n_s). \tag{38}$$

Using the diffusion coefficient defined by Eq. (2), and $r_s \approx r_{\mathrm{RD}}$ from Eq. (36), Eq. (38) gives

$$Gt_{cs} \approx \frac{4\pi k r_{\mathrm{RD}}^4}{9\Omega N_d(1 + 2/r_{\mathrm{RD}}^k N_d)}. \tag{39}$$

For $n_s = 10^4$, which in the case of molybdenum ($\Omega = 10.17$ A^3) corresponds to $r_{\mathrm{RD}} = 2.9$ nm, $k^2 = 2.0\times 10^{15}$ m^{-2}, and $N_d = 100$, it follows from Eq. (39) that the characteristic dose $Gt_{cs} \approx 4$ dpa. When the stochastic fluctuations dominate the kinetics of random voids, while the evolution of the RIF voids is determined by the mean-field growth, the value of Gt_{cs} is also the characteristic dose required for the void lattice formation. Thus, in agreement with experimental observations,[3,48] the nominal dose Kt_{cs} for void lattice formation is on the order of 10 NRT dpa ($G/K \cong 0.3$[43,45]).

Taking into account expression (8) for ε_v', Eq. (35) can also be rewritten in the form

$$\frac{dn}{dt} = \frac{3n^{1/3}G}{a^2k^2}\left\{\frac{\rho}{k^2}\left((1-\varepsilon_i)(Z-1) - \frac{\varepsilon_{i0}\lambda k^2}{2}(an^{1/3}\Phi - \pi d) - \frac{q(n_0 - n_{\min})k^2}{N_d\rho}\right) + \frac{\varepsilon_{i0}\lambda k_c^2}{2}\left[\frac{4\pi(N_{\mathrm{RIF}}\bar{r}_{\mathrm{RIF}}^2\Phi_{\mathrm{RIF}} + N_{\mathrm{RD}}\bar{r}_{\mathrm{RD}}^2)}{k_c^2} - an^{1/3}\Phi\right]\right\}. \tag{40}$$

One may then notice that the term $0.5\varepsilon_{i0}\lambda k^2 r_{\mathrm{RIF}}\Phi_{\mathrm{RIF}}$ in Eq. (40) is approximately equal to $\varepsilon_i \sim 10^{-2}$ [see Eq. (34)]. Thus, depending on the actual values of the dislocation bias $(Z-1)$ and the effective diameter of absorption d of crowdions by dislocations, subsequent growth of voids in a void lattice by two to three times may indeed lead to the saturation of void swelling, which is often observed experimentally.[48] Comparing the dislocation bias term and the third term in the round brackets of Eq. (40) indicates that the swelling may become saturated when the void sink becomes sufficiently large compared to the total dislocation density $[k_c^2/\rho \cong N_d(Z-1)/q]$. However, such a possibility should be considered with care, because a similar term with opposite sign would also arise from the generation of sessile interstitial clusters in collision cascades,[36] but has not been taken into account. A separate investigation is needed to resolve the issue of void swelling saturation during the void lattice formation.

Anyway, it is clear that Eq. (40) does not require swelling saturation as a necessary condition for void lattice formation. What is really necessary is a sufficiently high density of small voids, with average growth rate reduced so much that void growth can occur essentially by feeding on each other, i.e., when void coarsening becomes a dominant mode in the evolution of the void ensemble. This is consistent with the occasional observation of continued void growth after a void lattice has formed.[49] It should also be noted that, when $\rho/k_c^2 \approx 10^{-2}$, it is difficult to distinguish experimentally between swelling saturation and very low swelling rate.

The results of the foregoing section are derived based on a constant saturation size. Strictly speaking, the size defined by Eq. (36) is time dependent. From Eqs. (35) and (40), the characteristic time t_r for the average void radius to change can be estimated as

$$Gt_r \approx r^2k^2\frac{k^2}{(Z-1)\rho}. \tag{41}$$

The ratio of the two characteristic times t_{cs}/t_r is given by

$$\frac{t_{cs}}{t_r} \approx \frac{n_s}{3(r_skN_d+2)}\frac{(Z-1)\rho}{k^2}. \tag{42}$$

For $\rho/k^2 \approx 10^{-2}$, $Z-1=0.05$, $k^2=2\times10^{15}$ m^{-2}, $n_s=10^4$, this ratio is $\sim 1.1\times10^{-1} \ll 1$. This means that the change of the average void size is slow compared to the stochastic void coarsening process, thus justifying the present approach within the adiabatic approximation.

The case of dynamic crowdions can also be considered. Unlike static crowdions, which undergo one-dimensional random walk along the crystallographic close-packed directions, dynamic crowdions propagate along these directions via the displacement collision sequences. Let $F(l)$ be the probability that a dynamic crowdion may cover a distance larger than l, which is governed by an exponential law, i.e., $F(l)=\exp(-l/\lambda)$.[50] We can then write down an equation similar to Eq. (32) for the flux of dynamic crowdions received by the void

$$\left.\frac{dn}{dt}\right|_{\text{1D interstitials}} = -\frac{\pi r^2\lambda\varepsilon_{i0}G}{\Omega}\Phi = -\frac{3\lambda\varepsilon_{i0}G}{4a}n^{2/3}\Phi. \tag{43}$$

Here

$$\Phi_{\text{RIF}} = \frac{(2M-m)(1-\exp(-2L/\lambda))+m(1-\exp(-L/\lambda))}{2M}. \tag{44}$$

The foregoing results for the static crowdions can then be easily translated to the case of dynamic crowdions. Since $\tanh(x/2)/[1-\exp(-x)]=[1+\exp(x)]^{-1}<1$, the difference between these two cases is just quantitative. Compared to the static crowdions, the mean free path of the dynamic ones should be somewhat longer in order to have the same quantitative effect on the evolution of the void ensemble.

B. Crowdion clusters

In the foregoing section, the 1D flux of interstitials received by a void is determined by the fraction of interstitials directly produced in the CSCs of this void [Eq. (32)]. In the case of crowdion clusters that change directions from time to time, clusters produced outside the CSCs may also enter a void through one of its CSCs. With this additional contribution taken into account, the flux of 1D interstitials received by the void is given by (Appendix B)

$$\left.\frac{dn}{dt}\right|_{\text{1D interstitials}} = -\frac{r^2\Omega^{-1}\varepsilon_{i0}G\Phi}{[N_{\text{RIF}}\bar{r}^2_{\text{RIF}}\Phi_{\text{RIF}}+N_{\text{RD}}\bar{r}^2_{\text{RD}}+\rho d/4]} = -\frac{3\varepsilon_{i0}Gn^{2/3}\Phi}{4\pi a[N_{\text{RIF}}\bar{r}^2_{\text{RIF}}\Phi_{\text{RIF}}+N_{\text{RD}}\bar{r}^2_{\text{RD}}+\rho d/4]}, \tag{45}$$

where Φ and Φ_{RIF} have the same meaning as in the static crowdion case. As a result, the evolution equation of the void size in the mean-field approximation takes the form

$$\frac{dn}{dt} = \frac{3n^{1/3}G}{a^2k^2}\left(\left\{\frac{\rho}{k_c^2}\left((1-\varepsilon_{i0})(Z-1) - \frac{\varepsilon_{i0}k_c^2an^{1/3}\Phi}{4\pi(N_{\text{RIF}}\bar{r}^2_{\text{RIF}}\Phi_{\text{RIF}}+N_{\text{RD}}\bar{r}^2_{\text{RD}})}\times\left(1-\frac{\pi dk_c^2}{4\pi(N_{\text{RIF}}\bar{r}^2_{\text{RIF}}\Phi_{\text{RIF}}+N_{\text{RD}}\bar{r}^2_{\text{RD}})}\right)\right)\right\} - \varepsilon_v' + \varepsilon_{i0}\left[1-\frac{k_c^2an^{1/3}\Phi}{4\pi(N_{RIF}\bar{r}^2_{\text{RIF}}\Phi_{\text{RIF}}+N_{\text{RD}}\bar{r}^2_{\text{RD}})}\right]\right). \tag{46}$$

In deriving Eq. (46) we have assumed that $\rho/k_c^2 \ll 1$. The saturated void size in this case also obeys Eq. (36) as for the single crowdions. We note that here the conversion of 1D mobile clusters to 3D mobile ones does not occur, and the fraction of interstitials that do not participate in the conventional 3D migration is $\varepsilon_i=\varepsilon_{i0}$. Following the results of Sec. III A, crowdion clusters may also similarly produce void ordering if $\varepsilon_{i0}\sim 1\%$.

The foregoing discussion shows that the effects of single crowdions and crowdion clusters are essentially similar, the main difference being due to variations in the functional dependence of ε_i on the mean-free path λ. In this regard, we note that ε_i is independent of λ in the case of crowdion clusters. According to Eq. (46), when $\varepsilon_{i0}\sim 1\%$, the mean-free paths of crowdion clusters can be several times larger than the average distance between voids without seriously affecting the kinetics of the void ensemble. This resolves the controversy in the requirements for the mean free path of crowdion clusters, discussed earlier in the Introduction.

The kinetics of the void ensemble changes fundamentally when $\varepsilon_{i0}\sim 100\%$, as it is assumed in various Monte Carlo simulations.[24–26] It can be shown that the mean-field approximation, Eq. (46), gives a good description of the evolution of the void ensemble in this case, and the stochastic effects are much too weak to have any significant influence. Indeed, an assumed stationary solution of Eq. (46)

$$r_{\text{RD}} = r_{\text{RIF}}\Phi_{\text{RIF}}, \tag{47}$$

together with the conditions $\bar{r}^2_{\text{RIF}}=(r_{\text{RIF}})^2$ and $\bar{r}^2_{\text{RD}}=(r_{\text{RD}})^2$ that must be satisfied at saturation, reduce Eq. (46) to

$$\frac{dn}{dt} = \frac{3n^{1/3}\varepsilon_{i0}G}{a^2k^2}\left\{\frac{\rho}{k_c^2}\left(\frac{(1-\varepsilon_{i0})(\bar{Z}-1)}{\varepsilon_{i0}} - \left(1-\frac{\pi d}{r_{\text{RD}}}\right)\right) + \left(1+\frac{\rho}{k_c^2}\left(1-\frac{\pi d}{r_{\text{RD}}}\right)\right)\left[1-\frac{an^{1/3}\Phi}{r_{\text{RD}}}\right]\right\}, \tag{48}$$

which has the following stationary solution that can be shown to be stable

$$r_{\text{RD}} = \frac{\pi d}{[1-(\bar{Z}-1)(1-\varepsilon_{i0})/\varepsilon_{i0}]}. \tag{49}$$

Here

$$\bar{Z} = Z - \varepsilon_v' k_c^2/\rho(1-\varepsilon_{i0}). \tag{50}$$

Thus, when $\varepsilon_{i0} \sim 100\%$, random voids do not shrink, and the formation of void lattice can only occur through the spatial motion of voids to the lattice positions. However, it is demonstrated in Ref. 26 that the kinetics of the void ensemble in this case seems to be dominated by the coalescence of RIF voids induced either by the crowdions or the crowdion clusters, which precludes the formation of a stable lattice. The effect of void coalescence in the present framework will be discussed in the next section.

Simultaneously assuming $\varepsilon_{i0} \sim 100\%$ and $\lambda \gg L$ also leads to serious inconsistency with experimental observations. Indeed, when $\varepsilon_{i0} \sim 100\%$, Eq. (47) dictates that the ratio of the asymptotic sizes of the nonaligned to aligned voids is equal to $\tanh(L/2\lambda) \cong L/2\lambda \ll 1$, when $\lambda \gg L$. On the other hand, experimental observations at lower temperatures show that the diameter of the RIF voids forming the lattice can be as small as 3–4 nm.[3,27] Then a large mean-free path for the interstitial clusters means the practical absence of all random voids. Referring to Eq. (49) for the asymptotic radius of the random voids, which is valid independent of the presence of the RIF voids, confirms that these voids are practically invisible when $\varepsilon_{i0} \sim 100\%$. This is contrary to experiments, in which random voids are observable, with average sizes that are at least not small compared to those of the aligned voids.[27]

IV. VOID COALESCENCE

The mechanism of void coalescence can be easily understood using Fig. 3. A nucleating void shown by the dashed circle will receive a smaller 1D flux of interstitials on its right side than on the left one, due to the sharing of the interstitial supply. As a result, it will move to the right, towards its aligned neighbor. According to the MC simulation in Ref. 26, both voids will eventually coalesce. In the case of single crowdions, which actually corresponds to the methodology used in the MC simulation,[26] the difference in the crowdion fluxes $\Delta \dot{P}_1$ received by the left and right sides of the central void can be calculated from Eq. (31)

$$\Delta \dot{P}_1 = \frac{\varepsilon_{i0} G \pi r^2 \lambda}{M\Omega}[1 - \tanh(L/2\lambda)]. \tag{51}$$

Thus, the velocity v of the center of gravity of the void towards the neighbor on the right side is equal to

$$v = \frac{3\varepsilon_{i0} G \lambda}{8M}[1 - \tanh(L/2\lambda)], \tag{52}$$

from which the dose Gt_{cls} required for an aligned void to move a distance equal to its radius r_{RIF} can be estimated

$$Gt_{cls} \cong \frac{8M}{3\varepsilon_{i0}[1 - \tanh(L/2\lambda)]}\frac{r_{\mathrm{RIF}}}{\lambda}. \tag{53}$$

For $r_{\mathrm{RIF}}/\lambda \approx 10^{-1}$, $\varepsilon_{i0} \approx 10^{-1}$, $M=4$ in the case of a bcc lattice, and $\tanh(L/2\lambda) \cong 0.5$, this dose is approximately 20 dpa, which is significantly larger than the characteristic dose required for the void lattice formation $Gt_{cs} \approx 4$ dpa. It has been shown[5(b)] that once the void lattice is formed, it is stable with respect to displacements. It can be also shown that to prevent coalescence with any of the nearest aligned neighbor it is sufficient for each lattice void to have four nearest void lattice positions occupied by other voids, when its center of gravity is still inside the shaded area[51] (Fig. 3). Therefore, in the present framework the coalescence of aligned voids is not expected to have a significant effect during void lattice formation.

V. DISCUSSION

By taking into account the effect of the noise in the kinetics due to stochastic fluctuations of the point defect fluxes, our present formulation can be considered as a formal extension of the standard rate theory. Thus, when very few sessile interstitial clusters are directly produced in collision cascades, which is probably the case in bcc metals,[20,21,23,43] void growth in the present formulation is driven solely by the dislocation bias. On the other hand, if a significant fraction of interstitials generated in collision cascades is in the form of immobile clusters, such as in fcc copper,[20–23] the major driving force for void swelling in the peak swelling regime comes from the "production bias."[52,36] In cases where the stochastic noise is small relatively to the growth rate, similarities in the behavior of a void ensemble can be found between the predictions of the mean-field theory and the present theory. Otherwise, the mean-field theory breaks down and important differences show. In this regard, the roles played by variables such as the dislocation density, and the nature of the damage are of particular importance.

Within the mean-field approximation, when the average net vacancy flux due to the dislocation bias is sufficiently low, even a small fraction of 1D moving self-interstitials ($\varepsilon_i \sim 10^{-2}$) may seriously affect the behavior of the void ensemble. Indeed, according to Eqs. (35), (40), and (46), when the swelling rate is below 0.1%/NRT dpa, i.e., $(Z-1)\rho/k^2 < 3 \times 10^{-3}$ ($G/K \cong 0.3$,[43,45]), void growth proceeds more at the expense of each other rather than from the net vacancy supply resulting from the dislocation bias. More precisely, voids with smaller-than-average sizes receive a smaller 1D self-interstitial flux and grow at the expense of the larger ones [see the term in square brackets in Eqs. (40) and (46)]. This happens to both the aligned and nonaligned voids, so that in a mixture both components will asymptotically grow towards saturation at their respective characteristic sizes as governed by the mean-field approximation.

Furthermore, the mean-field rate equation for the average void size of a system of ordered voids is practically the same as that for a system of random voids [i.e., as defined by the term $\propto \rho/k_c^2$ in Eqs. (40) and (46)]. As observed experimentally,[3,27,47,48] the time and temperature dependences of the average void sizes for both the random and the ordered void ensembles are very similar. Only their absolute values may be different, which depends on the actual ratios of the dislocation and the void sink strengths. Since a higher void concentration is required for the void lattice to form, the sizes of voids in the lattice then have to be smaller than the

average sizes of the random voids at the same temperature.[3]

The behavior of the void ensemble in the mean-field approximation is fundamentally different if the fraction of the self interstitials in the form of 1D diffusing crowdion clusters is too large [i.e., $\varepsilon_{i0} \gg (Z-1)$]. In this case, void growth is not controlled by the conventional dislocation bias, but by the stronger DAD bias.[19] As the random voids grow to a radius $r \approx \pi d$ [Eq. (49)], the reaction rate of crowdion clusters with them becomes comparable to the reaction rate with the dislocations, causing void growth to saturate. The saturation also takes place for the aligned voids, only at a larger size [$r = \pi d / \tanh(L/2\lambda)$]. When $\varepsilon_{i0} \gg (Z-1)$, stochastic fluctuations do not play an important role in the evolution of the void ensemble, and, consequently, there is no mechanism via which the shrinkage of nonaligned voids can occur. Thus, the size of nonaligned voids indeed saturates at the value dictated by the mean-field approximation. As it is demonstrated by the MC simulation[26] the coalescence between the aligned voids also creates a strong barrier against the formation of the void lattice through the motion of the random voids to their nearby lattice positions. Accordingly, one may conclude that under the condition $\varepsilon_{i0} \gg (Z-1)$ void lattice formation indeed becomes difficult.

In the cases discussed in the foregoing, the stationary states according to the mean-field description are stable, and in such cases, void lattices do not form. Due to the nonlinear nature of the kinetics involved, the stability of the stationary states is only conditional. As it is shown in the present paper, if ε_i is less than 1% the noise in the point-defect fluxes has a profound effect on the growth behavior of the random voids when the swelling rate drops below 0.1%/NRT dpa (e.g., due to a high density of voids). If the average void size is also sufficiently small, the kinetics of the random voids is dominated by the stochastic fluctuations and the asymptotic states in mean-field description becomes unstable. The resulting noise-induced phase transition[41] transforms the collection of random voids from a long-life phase to a short-life phase. The majority of the random voids then shrink away, leaving the aligned ones to form a void lattice, as the winning species in the Darwinian competition.

At this point, we note that, although a high void-number density due to a low nucleation barrier produces a low swelling rate and a small average void size, this is by no means the only way such a condition can be achieved. Other factors such as impurity segregation to the void surfaces may also cause a reduced net vacancy flux to the voids to produce a similar effect leading to the instability of a homogeneous void distribution.

Because of the strong dependence of void nucleation probability on the magnitude of the net vacancy flux, the nucleation of voids in the void-lattice positions can indeed be realized, as often observed experimentally, even at a void swelling below 1%. The estimated dose ($\sim$10 NRT dpa) required for the completion of the void lattice formation process is also consistent with experimental observations. Since the aligned voids are shown to nucleate in the close proximity of the lattice positions, void coalescence induced by the 1D SIA transport is not expected to be important.[5,51]

It is beyond the scope of the present paper to consider in detail how different modes of 1D SIA transport can affect the behavior of the void ensemble, and to compare these effects with available experimental data. Besides, single crowdions or crowdion clusters do not seem to be the only feasibilities. According to MD and *ab initio* calculations,[53–55] the $\langle 111 \rangle$ dumbbell is found to be the most stable structure of self-interstitials in vanadium. In other MD calculations using many-body potentials, $\langle 11\bar{2}0 \rangle$ dumbbells/crowdions are also found to be the most stable single-interstitial structures in HCP zirconium and titanium.[56–58] The activated states for migration have an extremely low barrier. However, the activation energy for the dumbbell/crowdion rotation to the equivalent direction is about 2 to 4 tenths of an eV. Thus, at elevated temperatures the diffusion motion of such dumbbell will be mostly three dimensional, although a low probability of the occasional one-dimensional diffusion for sufficiently long distances may still exist. In this case the reaction kinetics will be different from that of single crowdions or crowdion clusters, and requires a separate investigation. Despite that, the present investigation obviously reconfirms an important role played by the one-dimensional interstitial diffusion in the void lattice formation.

Vacancy emission is neglected in this paper. Void coarsening is entirely noise induced by the stochastic fluctuations. Since the so called void "hyperlattices" in Al[59,60] with a lattice constant of about 200 nm are observed at temperatures for which vacancy emission is an important factor in the void evolution, the present approach is, straightly speaking, not applicable to such cases. However, conventional void coarsening due to vacancy emission has been shown to be able to produce spatial ordering in a void ensemble at higher temperatures when vacancy emission from voids becomes important.[10] Because of the orientation degeneracy of the kinetic model in those cases, the role of one-dimensional self-interstitial diffusion in the hyperlattice formation needs further consideration.

VI. SUMMARY AND CONCLUSIONS

In the present paper the effect of one-dimensionally migrating self-interstitials on the evolution of a void ensemble under irradiation by energetic particles is investigated. To properly consider the effects of void nucleation in the evolution, stochastic fluctuations in the point-defect fluxes, due to both the random nature of migratory jumps and cascade initiations, are taken into account. The kinetic equation we use for the void evolution, which keeps the effects of the stochastic fluctuations in its simplest approximation, has the form of the Fokker-Planck equation.

When the average distance between randomly distributed voids is comparable with the mean free path of the one-dimensional migrating self-interstitials, there is a significant reduction in the one-dimensional interstitial flux in the regions where voids aligned along the close-packed directions are in proximity with each other. As a result, the aligned voids receive a higher net vacancy flux. We have shown that, due to the high sensitivity of void nucleation probability to the net vacancy flux, the population of aligned voids can become dominant sinks when the void swelling is still below 1%. Moreover, nucleation of the aligned voids with high sink

strength not only suppresses further nucleation of the random voids, but also enhances the stochastic shrinkage of the already existing ones, leaving only the aligned voids behind to form a void lattice.

Since the flux of the self-interstitials moving one dimensionally along the crystallographic close-packed directions towards a void is proportional to the surface area of the void, voids with smaller sizes receive smaller 1D flux of interstitials. This is true for both aligned and nonaligned voids. We have shown that the effective shrinkage of nonaligned voids requires that the fraction of 1D moving interstitials ε_i be at most about 1%. A much higher fraction causes the small random voids to receive a high net vacancy flux, which prevents them from the shrinkage. It is also found that at a much higher fraction, the predicted behavior of the void ensemble does not agree with that observed experimentally when void lattices are formed.

ACKNOWLEDGMENTS

The authors are grateful for funding support by the Hong Kong Research Grant Council (research grants PolyU 5322/04E, 5309/03E and 5312/03E).

APPENDIX A: SOLUTION OF THE KINETIC EQUATION

The stationary form of Eq. (12) can be written as

$$\frac{\partial}{\partial n}\left\{V(n)-\frac{\partial}{\partial n}D(n)\right\}f(n)=j_0\delta(n-n_0). \tag{A1}$$

The solution $\rho(n)$ of the homogeneous equation ($j_0=0$) is obviously

$$\rho(n)=\frac{1}{D(n)}\exp\left[\int_{n_{\min}}^{n}\frac{V(n')}{D(n')}dn'\right]. \tag{A2}$$

Since the void-size distribution should be continuous at $n=n_0$, the stationary solution $f(n)$ of Eq. (A1) with the boundary conditions (10) and (11) can be written as

$$f(n)=A\rho(n)\int_{n_{\min}}^{n}\frac{dn'}{D(n')\rho(n')},\quad \text{for } n_{\min}<n<n_0, \tag{A3}$$

$$f(n)=A\rho(n)\int_{n_{\min}}^{n_0}\frac{dn'}{D(n')\rho(n')},\quad \text{for } n>n_0, \tag{A4}$$

where A is a constant to be determined.

Integrating Eq. (A1) over the infinitesimal interval around the point $n=n_0$, we have

$$J(n_0+0)-J(n_0-0)=j_0. \tag{A5}$$

Here $J(n)$ is the flux of voids in the space of sizes, i.e.

$$J(n)=\left\{V(n)-\frac{\partial}{\partial n}D(n)\right\}f(n). \tag{A6}$$

From Eqs. (A3) and (A4) it is easy to show that $J(n>n_0)=0$ and $J(n<n_0)=-A$. As a result, $A=j_0$, so that for $n>n_0$

$$f(n)=\frac{j_0}{D(n)}\exp\left[\int_{n_{\min}}^{n}\frac{V(n')}{D(n')}dn'\right]\times\int_{n_{\min}}^{n_0}\exp\left[-\int_{n_{\min}}^{n'}\frac{V(n'')}{D(n'')}dn''\right]dn'. \tag{A7}$$

Finally, using the mean value theorem for the second integral in (A7), we arrive at Eq. (12). Note also that with the boundary conditions (3) the derivative $\partial/\partial n[D(n)f(n,t)]$ at $n=n_{\min}$ measures the flux of voids $[-J(n_{\min})]$ shrinking below the minimum size, which is equal to j_0.

APPENDIX B: REACTION PROBABILITIES

Let us consider a random walker moving one-dimensionally along the direction between two absorbing traps at $x=0$ and $x=l$. The probability $P(x,t|x_0)$ that a random walker originally at x_0 is found at a new position x after time t is given by the conventional diffusion equation

$$\frac{\partial P}{\partial t}=D_1\frac{\partial^2 P}{\partial x^2}-\frac{P}{\tau_c} \tag{B1}$$

with the boundary conditions

$$P(0,t|x_0)=P(l,t|x_0)=0. \tag{B2}$$

Further, the probability $P_a^{(0)}(x_0)$ for the absorption of 1D diffusing random walker by the trap at $x=0$ is determined by the corresponding flux integrated over time

$$P_a^{(0)}(x_0)=D_1\left[\frac{d}{dx}\int_0^{\infty}P(x,t|x_0)dt\right]_{x=0}. \tag{B3}$$

Averaged over the initial position x_0, the absorption probabilities are the same for both traps and can be calculated from the function

$$\tau(x)=\frac{1}{l}\int_0^l\int_0^{\infty}P(x,t|x_0)dtdx_0, \tag{B4}$$

which, in its turn, can be found from the stationary diffusion equation following directly from the definition (B4) and Eq. (B1)

$$-\frac{1}{l}=D_1\frac{d^2\tau(x)}{dx^2}-\frac{\tau(x)}{\tau_c}. \tag{B5}$$

The solution of Eq. (B5) with the zero boundary conditions is elementary and gives the following probability of absorption:

$$P_a=\left.D_1\frac{d\tau(x)}{dx}\right|_{x=0}=-\left.D_1\frac{d\tau(x)}{dx}\right|_{x=l}=\frac{\lambda}{l}\tanh(l/2\lambda). \tag{B6}$$

Since the mean free path λ is assumed to be comparable with the average distance between voids, at low void swelling ($S\sim 1\%$), $\tanh(l/2\lambda)\cong 1$ for the randomly distributed voids. In the case of void lattice formation dislocation density ρ is much smaller than the void sink strength, and this

approximation is assumed to be valid for the dislocations as well. In the calculations we also took into account that the cross section of dislocation lines $\rho d \sin\theta / s_\perp$ for a close-packed direction (here θ is the angle between the dislocation line and the close-packed direction) averaged over all possible line orientations gives $\pi\rho d/4s_\perp$ for the isotropic line distribution.[46] Thus, we arrive at Eqs. (32)–(34)

Unlike the static or dynamic crowdions, crowdion clusters produced outside of the void supply cylinder also contribute to the number of crowdion clusters in the cylinder and, consequently, can be absorbed by the corresponding void. To find the flux of 1D interstitials received by the void when clusters change the directions of their Burgers vectors, let us consider a "pipe" α with the length l_α and cross section $s_\perp$, which connects two absorbing traps separated by the distance l_α. From Eq. (B6), the probability p_α^0 that a crowdion cluster will be generated and then absorbed in this pipe before it changes the direction of its motion is equal to

$$p_\alpha^0 = 2s_\perp l_\alpha P_a(l_\alpha)/MV = \frac{2s_\perp \lambda}{MV} \tanh(l_\alpha/2\lambda), \tag{B7}$$

where V is the total volume considered. Therefore, the probability that a cluster generated in V will be absorbed before it changes the direction of motion is given by

$$\sum_\alpha p_\alpha^0 = \frac{2s_\perp \lambda}{MV} \sum_\alpha \tanh(l_\alpha/2\lambda), \tag{B8}$$

where the summation is over all "pipes" in the volume V. As a result, the probability p_α that a crowdion cluster generated in the volume V will be absorbed in the pipe V_α is determined by the following algebraic equation:

$$p_\alpha = p_\alpha^0 + \left[1 - \sum_{\alpha'} p_{\alpha'}^0\right] p_\alpha. \tag{B9}$$

Here the term in square brackets means the probability that a crowdion cluster will be absorbed after it changes the motion direction.

For a spherical void of the radius r its cross section for any given close-packed atomic direction is equal to $\pi r^2/s_\perp$. Summing up the probabilities p_α over all pipes, which are crossed by the void surface, we get that the probability for a crowdion cluster to be absorbed by the void is equal to

$$\frac{((2M-m)\tanh(L/\lambda) + m\tanh(L/2\lambda))}{M} \frac{\pi r^2 \lambda/V}{\sum_{\alpha'} p_{\alpha'}^0} \tag{B10}$$

in the case of aligned voids, and to

$$\frac{2\pi r^2 \lambda/V}{\sum_{\alpha'} p_{\alpha'}^0} \tag{B11}$$

in the case of randomly distributed voids.

Finally, grouping terms p_α^0 in the denominator, which correspond to the network dislocations, aligned and randomly distributed voids, and taking also into account that rate of cluster generation in V is given by $\varepsilon_{i0} GV/\Omega$, we obtain Eq. (45).

*Corresponding author; e-mail: chung.woo@polyu.edu.hk

[1] J. H. Evans, Nature (London) **229**, 403 (1971).
[2] A. M. Stoneham, in *The Physics of Irradiation Produced Voids*, Proc. Consult. Symp., Harwell Report AERE-R-7934, edited by R. S. Nelson (UK, Harwell, 1975), p. 319.
[3] K. Krishan, Radiat. Eff. **66**, 121 (1982).
[4] E. Johnson and L. T. Chadderton, Radiat. Eff. **79**, 183 (1983).
[5] C. H. Woo and W. Frank, J. Nucl. Mater. **137**, 7 (1985); C. H. Woo and W. Frank, *ibid.* **140**, 214 (1986); C. H. Woo and W. Frank, *ibid.* **148**, 121 (1987).
[6] A. M. Stoneham, J. Phys. F: Met. Phys. **1**, 778 (1971).
[7] V. K. Tewery, J. Phys. F: Met. Phys. **3**, 1275 (1973).
[8] A. A. Lucas, Phys. Rev. B **7**, 3527 (1973).
[9] K. Krishan, Philos. Mag. A **45**, 401 (1982).
[10] E. A. Koptelov and A. A. Semenov, J. Nucl. Mater. **170**, 178 (1990).
[11] E. A. Koptelov and A. A. Semenov, in *Effects of radiation on materials*: 15th International Symposium, ASTM STP 1125, edited by R. E. Stoller, A. S. Kumar, and D. S. Gelles (USA, Philadelphia, 1992), p. 583.
[12] D. Walgraef, J. Lauzeral, and N. M. Ghoniem, Phys. Rev. B **53**, 14782 (1996).
[13] D. Walgraef and N. M. Ghoniem, Phys. Rev. B **67**, 064103 (2003).
[14] E. A. Koptelov and A. A. Semenov, Phys. Status Solidi A **93**, K33 (1986).
[15] A. J. E. Foreman, *Harwell Report AERE-R-7135* (UK, Harwell, 1972).
[16] J. H. Evans, J. Nucl. Mater. **119**, 180 (1983).
[17] J. H. Evans, J. Nucl. Mater. **132**, 147 (1985).
[18] P. Hähner and W. Frank, Solid State Phenom. **23&24**, 203 (1992).
[19] C. H. Woo, J. Nucl. Mater. **159**, 237 (1988).
[20] D. J. Bacon, F. Gao, and Yu. N. Osetsky, J. Nucl. Mater. **276**, 1 (2000).
[21] Yu. N. Osetsky, D. J. Bacon, A. Serra, B. N. Singh, and S. I. Golubov, J. Nucl. Mater. **276**, 65 (2000).
[22] Yu. N. Osetsky, D. J. Bacon, and B. N. Singh, J. Nucl. Mater. **307&311**, 866 (2002).
[23] D. J. Bacon, Yu. N. Osetsky, R. Stoller, and R. E. Voskoboinikov, J. Nucl. Mater. **323**, 152 (2003).
[24] H. L. Heinish and B. N. Singh, J. Nucl. Mater. **307&311**, 876 (2002).
[25] H. L. Heinish and B. N. Singh, Philos. Mag. **83**, 3661 (2003).
[26] J. H. Evans, Philos. Mag. **85**, 1177 (2005).
[27] V. K. Sikka and J. Moteff, J. Nucl. Mater. **54**, 325 (1974).
[28] K.-Y. Liou, H. V. Smith, Jr., P. Wilkes, and G. L. Kulcinski, J. Nucl. Mater. **83**, 335 (1979).
[29] B. A. Loomis and S. B. Gerber, J. Nucl. Mater. **102**, 154 (1981).
[30] S. L. Dudarev, A. A. Semenov, and C. H. Woo, Phys. Rev. B **67**,

094103 (2003).
[31] S. L. Dudarev, A. A. Semenov, and C. H. Woo, Phys. Rev. B **70**, 094115 (2004).
[32] A. M. Ovcharenko, C. H. Woo, and A. A. Semenov, J. Nucl. Mater. **341**, 201 (2005).
[33] A. A. Semenov and C. H. Woo, Appl. Phys. A **69**, 445 (1999).
[34] A. A. Semenov and C. H. Woo, J. Nucl. Mater. **233-237**, 1045 (1996).
[35] P. Ehrhart, K. H. Robrock, and H. R. Schober, *Basic Defects in Metals, in Physics of Radiation Damage in Crystals*, edited by R. A. Johnson and A. N. Orlov (Elsevier, Amsterdam, 1986).
[36] A. A. Semenov and C. H. Woo, Philos. Mag. **67**, 193 (1998).
[37] B. L. Eyre and A. E. Barlett, J. Nucl. Mater. **47**, 143 (1973).
[38] J. F. Stubbins, J. Moteff, and A. Taylor, J. Nucl. Mater. **101**, 64 (1981).
[39] V. F. Zelensky, I. M. Nekludov, L. S. Ozhigov, *Some Problems in the Physics of Radiation Damage in Materials* (Naukova Dumka, Kiev, 1979).
[40] U. M. Gösele, Prog. React. Kinet. **13**, 63 (1984).
[41] W. Horsthemke and R. Lefever, *Noise-Induced Transitions* (Springer, Berlin, 1984).
[42] A. A. Semenov and C. H. Woo, Phys. Rev. B **66**, 024118 (2002).
[43] K. Morishita and T. Diaz de la Rubia, J. Nucl. Mater. **271&272**, 35 (1999).
[44] A. Almazouzi, M. Victoria, M. J. Caturla, and T. D. de la Rubia, EPFL Supercomputing Review, No 10, Swiss Fed. Inst. of Technology, 10 (1998).
[45] R. Pasianot, M. Alurralde, A. Almazouzi, and M. Victoria, Philos. Mag. A **82**, 1671 (2002).
[46] S. L. Dudarev, Phys. Rev. B **62**, 9325 (2000).
[47] B. A. Loomis, A. Taylor, and S. B. Gerber, J. Nucl. Mater. **56**, 25 (1975).
[48] B. A. Loomis, S. B. Gerber, and A. Taylor, J. Nucl. Mater. **68**, 19 (1977).
[49] J. L. Brimhall and E. P. Simonen, J. Nucl. Mater. **52**, 323 (1974).
[50] M. Zaiser, W. Frank, and A. Seeger, Solid State Phenom. **23&24**, 221 (1992).
[51] A. A. Semenov, C. H. Woo, and W. Frank, Philos. Mag. Lett. **85**, 563 (2005).
[52] C. H. Woo and B. N. Singh, Phys. Status Solidi B **159**, 609 (1990); , Philos. Mag. A **65**, 889 (1992).
[53] S. Han, L. A. Zepeda-Ruiz, G. J. Ackland, and D. J. Srolovits, Phys. Rev. B **66**, 220101 (2002).
[54] L. A. Zepeda-Ruiz, S. Han, D. J. Srolovits, and R. Car, Phys. Rev. B **67**, 134114 (2003).
[55] S. Han, L. A. Zepeda-Ruiz, G. J. Ackland, R. Car, and D. J. Srolovits, J. Appl. Phys. **93**, 3328 (2003).
[56] C. H. Woo, Hanchen Huang, and W. J. Zhu, Appl. Phys. A **76**, 101 (2003).
[57] M. Wen, C. H. Woo, and Hanchen Huang, J. Parenter. Drug Assoc. **7**, 97 (2000).
[58] R. C. Pasianot and A. M. Monti, J. Nucl. Mater. **264**, 198 (1999).
[59] A. Risbet and V. Levy, J. Nucl. Mater. **50**, 116 (1974).
[60] A. Horsewell and B. N. Singh, Radiat. Eff. **102**, 1 (1987).